HHS Public Access

Author manuscript

Transl Stroke Res. Author manuscript; available in PMC 2024 August 01.

Published in final edited form as:

Transl Stroke Res. 2024 August ; 15(4): 831–843. doi:10.1007/s12975-023-01172-2.

Central IRF4/5 Signaling Are Critical for Microglial Activation and Impact on Stroke Outcomes

Conelius Ngwa[1], **Abdullah Al Mamun**[1], **Shaohua Qi**[1], **Romana Sharmeen**[1], **Maria P. Blasco Conesa**[1], **Bhanu P. Ganesh**[1], **Bharti Manwani**[1], **Fudong Liu**[1]

[1]Department of Neurology, McGovern Medical School, The University of Texas Health Science Center at Houston, Houston, TX 77030, USA

Abstract

Microglia and monocytes play a critical role in immune responses to cerebral ischemia. Previous studies have demonstrated that interferon regulatory factor 4 (IRF4) and IRF5 direct microglial polarization after stroke and impact outcomes. However, IRF4/5 are expressed by both microglia and monocytes, and it is not clear if it is the microglial (central) or monocytic (peripheral) IRF4-IRF5 regulatory axis that functions in stroke. In this work, young (8–12 weeks) male pep boy (PB), IRF4 or IRF5 flox, and IRF4 or IRF5 conditional knockout (CKO) mice were used to generate 8 types of bone marrow chimeras, to differentiate the role of central (PB-to-IRF CKO) vs. peripheral (IRF CKO-to-PB) phagocytic IRF4-IRF5 axis in stroke. Chimeras generated from PB and flox mice were used as controls. All chimeras were subjected to 60-min middle cerebral artery occlusion (MCAO) model. Three days after the stroke, outcomes and inflammatory responses were analyzed. We found that PB-to-IRF4 CKO chimeras had more robust microglial pro-inflammatory responses than IRF4 CKO-to-PB chimeras, while ameliorated microglial response was seen in PB-to-IRF5 CKO vs. IRF5 CKO-to-PB chimeras. PB-to-IRF4 or IRF5 CKO chimeras had worse or better stroke outcomes respectively than their controls, whereas IRF4 or 5 CKO-to-PB chimeras had similar outcomes compared to controls. We conclude that the central IRF4/5 signaling is responsible for microglial activation and mediates stroke outcomes.

Keywords

Chimera; Inflammation; IRF; Microglia; Monocytes; Stroke

✉Fudong Liu, Fudong.Liu@uth.tmc.edu.

Author contribution C.N. and A.A.M: project conception and design, conducting of experiments, acquisition of data, analysis, and interpretation of data, and manuscript writing. S.Q., M.P.B.C, and B.P.G: conducting experiment and acquisition of data and analysis. R.S.: mouse breeding and colony maintenance. B.P.G, B.M., and F.L.: contributed to conception and design, interpretation of data, and manuscript writing. All authors have read and approved the final version of the manuscript.
Conelius Ngwa and Abdullah Al Mamun contributed equally to this research.

Supplementary Information The online version contains supplementary material available at https://doi.org/10.1007/s12975-023-01172-2.

Competing interests The authors declare no competing interests.

Ethical Statement All studies were conducted in accordance with NIH guidelines for the care and use of laboratory animals and approved by the Institutional Animal Care and Use Committee (IACUC) of the University of Texas Health Science Center at Houston McGovern Medical School.

Introduction

Post-stroke inflammation is characterized mainly by the microglial response and brain infiltration of peripheral leukocytes, in which microglial activation plays a central role [1–3]. Microglia respond to ischemic injury and polarize toward two phenotypes: anti- and pro-inflammatory activation, a process tightly controlled by a bunch of intrinsic regulatory pathways [4–6]. Our previous studies have found that interferon regulatory factor 4 (IRF4) and IRF5 form a regulatory axis to synergistically mediate microglial activation after stroke, with the former directing anti-inflammatory and the latter pro-inflammatory response [1, 3, 7]. However, the IRF4 and IRF5 signaling also exist in another type of phagocyte, i.e., monocytes or macrophages [8–10]. After a stroke, the circulating monocytes are also activated and infiltrate into the ischemic brain to become macrophages, boosting the inflammatory response together with other immune cells including microglia. Whether monocytic IRF4 or IRF5 signaling also impacts ischemic stroke remains elusive. It is crucial to distinguish the role of microglial (central) vs. monocytic (peripheral) IRF4-IRF5 regulatory axis in stroke, given that cell-specific treatment has been proven more effective and less off-target effects than wholesale interventional therapies [11–13].

Distinguishing microglial vs. monocytic signaling has always been challenging, due to the fact that the two phagocytes share the same bio-markers to a great extent and have similar morphology and functions in the ischemic brain. The IRF4 or IRF5 microglial conditional knockout mouse model previously used was generated by gene flox and lysozyme Cre system [14–17]; however, lysozyme is expressed by both the microglia and monocyte. In this study, we have employed bone marrow (BM) chimera mice models [18, 19] to separately study the microglial vs. monocytic IRFs by using PepBoy (PB) mice [20]. Hematopoietic cells in PB mice express the Ptprca (CD45.1) [48] rather than the Ptprcb (CD45.2) that is however expressed by other C57BL/6 background strains including IRF4 and IRF5 flox or CKO mice. In chimeras generated by these mice, both the CD45.1 and CD45.2 common antigens in immune cells can be easily detected via flow cytometry. Therefore, the PB mice are useful donors or recipients in making BM chimeras to distinguish central (brain) vs. peripheral immune cells. With PB and IRF4 or 5 flox/CKO mice, we have generated a total of 8 BM chimeric mouse models and elucidated the roles of central vs. peripheral IRF4 and IRF5 signaling in stroke.

Materials and Methods

Animals

B6.SJL-Ptprc^{a}Pepc^{b}/BoyJ (PepBoy; PB) and IRF4 or 5 flox mice were purchased from The Jackson Laboratory. IRF4 or IRF5 CKO mice were generated by crossing IRF4/5 flox with LysMcre mice (JAX# 018956) as validated in [1]. All mice were group-housed under pathogen-free conditions with a 12-to-12-h day-night cycle and had access to food and water ad libitum. Mice were randomly chosen and used after they were examined free of aberrations or other abnormalities. All studies were conducted in accordance with NIH guidelines for the care and use of laboratory animals and approved by the Institutional Animal Care and Use Committee (IACUC) of the University of Texas Health Science Center at Houston McGovern Medical School.

BM Chimeric Mice Generation

BM chimeras were generated as previously described [18] with slight modifications. PB and IRF4/5 CKO or flox male mice (recipient; 8–12 weeks old) were lethally irradiated with two doses of 500 cGy radiation with a 3-h interval in an X-ray irradiator. Prior to irradiation, mice (body weight ≥ 20 g) were intraperitoneally injected with ketamine-xylazine (100 μL) for anesthesia. All mice undergoing X-ray irradiation were head-shielded to protect brain tissue from the lethal effect of the X-rays. After the irradiation, the recipient mouse was ready to receive bone marrow (BM) cells from the donor mouse. Sup. Fig. 1 shows the representative workflow for the BM chimera generation. First, the femur of the donor mouse (PB, IRF4/5 CKO or flox) was cut at both ends, and the bone marrow (BM) was harvested into a sterile polypropylene tube (50 mL) using a needled syringe (10 mL) filled with cold RPMI 1640 (ATCC, cat# 30–2001, VA, USA) solution. The BM was triturated and then passed through a 70-μm cell strainer (CELLTREAT Scientific Products, cat# 229,483, MA, USA). The strained cells were centrifuged at 1500 RPM for 5 min and at 4 °C. TAC was added to the cell pellet (2 mL) to lyse RBCs. Next, the suspension was diluted with cold RPMI 1640 (18 mL) and centrifuged at 1500 RPM for 5 min twice. The cell pellet was further suspended in cold PBS at the desired concentration ($1.5–2 \times 10^6$ cells/0.3 mL/per recipient mouse) and ready for Jugular vein injection (JVI) [21, 22] under the microscope. All experimental mice were maintained on neomycin sulfate antibiotics (2 g/L) in their drinking water, 1 day prior and 2 weeks after the X-ray irradiation and the JVI. Chimeras were allowed to reconstitute for 6–8 weeks after the JVI, and only those with > 90% donor-origin peripheral leukocytes (determined by FACS analysis of blood or spleen) were included in the study. The experimental grouping of this study is shown in Table 1.

Ischemic Stroke Model

Cerebral ischemia was induced in BM chimeras by reversible MCAO and under isoflurane anesthesia as previously described [7]. Briefly, a midline ventral neck incision was made, and unilateral MCAO was performed by inserting a 6–0 silicone-coated suture into the right internal carotid artery 6 mm from the internal carotid/ pterygopalatine artery bifurcation via an external carotid artery stump. Reperfusion was performed by withdrawing the suture 60 min after the occlusion. Rectal temperature was maintained at 36.5 ± 0.5 °C during surgery with an automated TC-1000 temperature-control feedback system (CWE, Inc., Ardmore, PA, USA). All mice were monitored on a daily basis and then sacrificed at 3 days of reperfusion. Sham-operated animals underwent the same procedure including exposure to isoflurane and a midline ventral neck incision, but the suture was not advanced into the MCA. Laser Doppler flowmetry (Moor Instruments Ltd, UK) was applied to measure CBF through the skull at the right temporal fossa [23]. Only the mice whose CBF showed a drop of over 85% of baseline after MCAO was included in the following experiments [24]. The mortality of the chimeras after MCAO was 20%. The size of the MCAO-induced infarct was measured by cresyl violet (CV) staining as described in [25].

Flow Cytometry

Flow cytometry was performed as previously described with modifications [26]. Briefly, PBS-perfused mice brains (ipsilateral hemisphere) were processed with a STANLEY razor

blade (cat# G0423622) to remove cerebella, pons, medulla oblongata, and olfactory bulb and then placed in complete Roswell Park Memorial Institute (RPMI) 1640 (Lonza) medium and mechanically and enzymatically digested in 150 μL collagenase/dispase (1 mg/mL) and 300 μL DNAse (10 mg/mL; both Roche Diagnostics) for 45 min at 37 °C with mild agitation. Harvested cells were washed and blocked with Mouse Fc Block (eBioscience) prior to staining with primary antibody-conjugated fluorophores: CD45.2-eF450_48045182, CD11b-AF488_47011282, and Ly6C-APC-eF780_47593282 (Invitrogen, USA) and CD45.1-eF450_110728, Ly6G-PE_127608, CD 68-APC_137008, and CD206-PE-cy7_141720 (BioLegend, CA, USA). For live/dead cell discrimination, a fixable viability dye, carboxylic acid succinimidyl ester (CASE-AF350, Invitrogen), was used. For intracellular cytokine staining, an ex vivo brefeldin A protocol was followed [27, 28], and an intracellular antibody mixture at 1:50 dilution containing TNF-α-PE-Cy7_25734982 (eBioscience, San Diego, CA, USA) and IL-1β-PE_12711482 (eBioscience), IL-4-APC_504106, and IL-10-PerCP-Cy5.5_505028 (BioLegend) was used for staining. Fluorescence minus ones (FMOs) and bead compensations were used for all staining experiments for both cell membrane and intracellular inflammatory mediators. Data were acquired on CytoFLEX-S (Beckman Coulter, CA, USA) or BD FACSMelody cytometer and analyzed using FlowJo (Tree Star Inc., OR, USA).

Neurologic Deficit Scores

Following MCAO, neurologic deficit scores (NDS) were measured as (0) no deficit, (1) forelimb weakness and torso turning to the ipsilateral side when held by the tail, (2) circling to the affected side, (3) unable to bear weight on the affected side, and (4) no spontaneous locomotor activity or barrel rolling as previously reported [29].

Corner Test

Corner test was performed to measure the sensorimotor deficit as previously described [7, 30]. Briefly, the mouse was placed between two cardboard pieces (each 30 cm × 20 cm × 1 cm), and the boards were gradually moved closer to the mouse from both sides to encourage the mouse to enter into a corner of 30° with a small opening along the joint between the two boards. When the mouse entered the deepest part of the corner, both sides of the vibrissae were stimulated by the two boards. Then, the mouse reared forward and upward and turned back at the affected side (right) to face the open end. Twenty trials were performed for each mouse, and the percentage of right turns was calculated. Only turns involving full rearing along either board were recorded.

Adhesive Removal Test

The test was to evaluate both somatosensory and motor function as in [31, 32]. Briefly, an adhesive tape circle (Ø 12 mm) was placed on the impaired, contralateral (left) forelimb paw. The mouse in the testing cage was observed, and the time to remove the adhesive tape (in seconds) was recorded for each mouse, with a time cap of 3 min.

Plasma and Brain Cytokine Levels by MultiPlex

Blood samples were obtained by cardiac puncture, and the plasma was collected as in [33]. Brain samples were prepared as in [34]. Cytokine levels were measured by the MultiPlex quantitative Bio-Plex Pro Mouse Cytokine 23-plex assay, according to the manufacturer's instruction (# M60009RDPD, Bio-Rad Laboratories, Hercules, CA, USA). All assays were performed in duplicates, and the mean of each assay was estimated using a standard curve.

Statistical Analysis

Data from individual experiments were presented as mean ± SD and assessed by Student's *t*-test or 2-way ANOVA with the Sidak post hoc test for multiple comparisons (GraphPad Prism software 9.5.0 (730), San Diego, CA, USA). $P < 0.05$ was considered statistically significant. The ordinal data of NDS was analyzed with the Mann–Whitney U test. Investigators were blinded to mouse strains for stroke surgery, behavioral testing, infarct, and inflammation analysis.

Results

Validation of the BM Chimera Model

All chimeras were made by using CD45.1 (PB) and CD45.2 (IRF flox and CKO) mice as BM donors or recipients. To validate the chimera model, we routinely examine the common antigen (CD45.1 or 0.2) in peripheral leukocytes in chimeras to determine if the BM has been reconstituted with a donor's BM. We performed flow cytometry on spleens from chimeras and stained cells with CD45.1 and 0.2 antibodies. FMO controls showed evident positive gating for CD45.1 and 0.2 (Fig. 1A, B). All chimeras made for the present study had over 95% peripheral leukocytes derived from the donor's BM. Figure 1C, D shows the common antigens of the spleen cells in a representative chimera in which the donor was CD45.2 and the recipient was CD45.1 (PB). The cells were over 95% CD45.2 positive (from the donor) and near null CD45.1 positive (the recipient), indicating that these cells were derived from the donor's BM and that the BM reconstitution in the recipients was successful.

Central IRF4-IRF5 Signaling Affects Microglial Activation

We have previously shown that IRF4 and IRF5 signaling from young adult and aged mice modulated microglial inflammatory responses and impacted stroke outcomes in an oscillating pattern [1, 7]. However, whether the effect is of central or peripheral IRF4/5 is not clear. To this end, we transplanted BM cells from PB to IRF4/5 CKO (controlled by PB-to-IRF4/5 flox), and from IRF4/5 CKO to PB mice (controlled by IRF4/5 flox-to-PB). The BM chimeric mice were then subjected to a 60-min MCAO. Three days after MCAO, flow cytometry was conducted to examine microglial cell membrane and intracellular inflammatory mediators. The gating strategy for microglia and other immune cells that infiltrated into the brain is shown in Sup. Fig. 2. CD68 and CD206 are the established pro- and anti-inflammatory cell membrane markers respectively [35, 36]. PB-to-IRF CKO chimeras were to examine central IRF signaling. The mean fluorescence intensity (MFI) of CD68 was significantly increased, but CD206 MFI decreased in PB-to-IRF4 CKO mice

compared to PB-to-IRF4 flox controls after stroke (Fig. 2A–C), and an opposite pattern was seen in PB-to-IRF5 CKO vs. PB-to-IRF5 flox chimeras (Fig. 2G–I). However, when we examine the peripheral IRF signaling (IRF CKO-to-PB chimeras), only CD68 showed similar changes (Fig. 2D–F, J–L). Interestingly, when we compared the MFI ratios of CKO over control chimeras (CKO/Flox) after stroke, we found that the CD68 ratio of PB-to-IRF4 CKO/PB-to-IRF4 flox (central manipulation) was significantly higher than the ratio of IRF4 CKO-to-PB/IRF4 flox-to-PB chimeras (peripheral manipulation) (Fig. 2M), and the ratio of CD206 showed the opposite pattern (Fig. 2N). The ratio of CD68 was significantly higher in IRF5 CKO-to-PB vs. PB-to-IRF CKO chimeras (Fig. 2O). The data clearly indicated that the central (but not peripheral) IRF4 or IRF5 signaling controls microglial activation after stroke.

Next, we examined intracellular inflammatory markers TNF-α/IL-1β (pro-inflammatory) and IL-10/IL-4 (antiinflammatory). Again, significant changes were mostly seen in PB-to-IRF CKO chimeras (central manipulation) (Fig. 3B, C, H; Sup. Fig. 3B), and IRF-to-PB (peripheral manipulation) only showed IL-1β change in one cohort (Fig. 3F). More importantly, when we quantified the MFI CKO/Flox ratios, the TNF-α ratio of PB-to-IRF4 CKO/PB-to-IRF4 flox was significantly higher (Fig. 3M), and the ratio of PB-to-IRF5 CKO/PB-to-IRF5 flox was lower (Fig. 3O) compared with the ratio in their peripheral counterparts (IRF4 or IRF5 to PB). The anti-inflammatory marker IL-10 ratio of PB-to-IRF4 CKO/PB-to-IRF4 flox was significantly lower than the ratio of IRF4 CKO-to-PB/IRF4 flox-to-PB (Sup. Fig. 3M). We also quantified CD68 and CD206 levels and ratios in infiltrating monocytes but found negative results except for CD68 levels in PB-to-IRF4 chimeras (Sup Fig. 4B). However, the CD68 MFI ratios were not significant in the PB-to-IRF4 chimeras compared with the IRF4-to-PB (Sup Fig. 4C). All other monocytic data were also negative (Sup. Fig. 4). All these data suggested that the central IRF signaling plays dominant roles in mediating phagocytic responses compared with the peripheral IRF signaling.

Central IRF4 Signaling Impacts on the Infiltration of Peripheral Immune Cells into the Ischemic Brain

Peripheral immune cell infiltration in the brain was also examined 3 days after the stroke. Flow cytometry data showed that the PB-to-IRF4 CKO (central IRF4 deleted) but not IRF4 CKO-to-PB (peripheral IRF deleted) chimeras had significantly more neutrophils and monocytes infiltrating in the ischemic brain compared with their controls (Fig. 4A, B), and IRF5 CKO chimeras did not change the leukocyte infiltration vs. flox controls (Fig. 4C, D). All data were from stroke mice, as sham mice have no infiltration of neutrophils and monocytes in the brain. These data suggested that central IRF4 signaling is critical in controlling brain infiltration of peripheral leucocytes after stroke.

Plasma and Brain Cytokine Levels After Stroke

To further study the impact of central vs. peripheral IRF4/5 signaling on immune responses, we also examined the plasma and brain cytokine levels with MultiPlex ELISA. Plasma levels of the pro-inflammatory cytokines IL-β, IL-6, IL-12p40, and TNF-α significantly increased (Sup. Fig. 5A–C, F), the anti-inflammatory cytokine IL-10 decreased (Sup. Fig. 5H) in the PB-to-IRF4 CKO vs. control chimeras after stroke, and the similar pattern

was seen in IRF4 CKO-to-PB chimeras vs. controls for some pro-inflammatory cytokines (IL-β, IL-12p40, IL-12p70, TNF-α) (Sup. Fig. 5I, K, L, N) and the anti-inflammatory cytokine IL-4 (Sup. Fig. 5O). Similarly, the brain levels of pro-inflammatory cytokines (IL-6, IL-p40, IL-12p70, TNF-α, IL-1β, MIP1-β) were significantly higher in chimeras with either central (PB-to-IRF4 CKO) or peripheral (IRF4 CKO-to-PB) IRF4 signaling compared to controls after stroke (Sup. Fig. 6). In IRF5 CKO–based chimeras, we found the opposite pattern in these cytokine levels in either plasma or brain but also without distinguished central vs. peripheral differences (Sup. Figs. 7&8). The consistent pattern in plasma or brain cytokine levels in mice with central vs. peripheral IRF signaling suggested that cytokines are produced and released from multiple cell populations but are not limited to phagocytes.

Central but not Peripheral IRF Signaling Contributes to Stroke Outcomes

To investigate the roles of central vs. peripheral IRF signaling in stroke outcomes, we measured histological and functional outcomes in these chimeras 3 days after MCAO. Significantly larger infarct volumes were found in all three brain areas (cortex, striatum, whole ipsilateral hemisphere) in PB-to-IRF4 CKO vs. control chimeras, and worse behavioral deficits were also seen in the PB-to-IRF4 CKO chimeras in NDS, corner test, and tape removal test (Fig. 5A–E). However, IRF4 CKO-to-PB chimeras only showed one positive result in the cortical infarct compared to their control, with no changes in the infarct in other brain areas and in neurobehavioral tests (Fig.5F–J). In IRF5 CKO–based chimeras, PB-to-IRF5 CKO chimeras had significantly smaller infarct size in the striatum/hemisphere, lower NDS scores, and less time to remove the tape than their control chimeras (Fig. 6A–E). Again, the deletion of peripheral IRF5 signaling failed to induce any significant differences in the infarct volumes and behavioral deficits compared to controls (Fig. 6F–J). These data strongly suggested that it is the central (but not peripheral) IRF signaling that impacts stroke outcomes.

Discussion

It is well known that IRF4 and 5 are expressed by both microglia and monocytes [1, 3, 7–9, 28, 37], and our previous study has shown that IRF4–5 regulatory axis affects immune responses and stroke outcomes [1, 7]. In the present study, we separately studied central (microglia) vs. peripheral (monocytes/macrophages) IRF4–5 axis using BM chimeras and revealed several important findings. Firstly, as we expected, the central IRF4/5 signaling is responsible for microglial activation; surprisingly, the peripheral IRF4/5 have minimal effect on monocytic activation after stroke. Secondly, the central IRF4 signaling not only mediates microglial activation but is also in control of peripheral immune cell infiltration into the ischemic brain. Thirdly, in correspondence with the roles of central vs. peripheral IRF signaling in phagocytic activation, the central IRF4–5 axis impacts stroke outcomes, whereas the peripheral IRF4/5 have a near null effect. Based on the literature, this is the first report of a comparison of the roles between central vs. peripheral IRF4–5 signaling in stroke, and our data showed that central IRF4/5 are more important in the pathophysiology of stroke than the peripheral signaling.

Upon cerebral ischemia, microglia are activated, and days later, peripheral monocytes are also activated and become macrophages infiltrating into the ischemic brain, further aiding in the post-stroke immune responses [38]. Microglia and monocytes are the major sources of inflammatory cytokines in neuroinflammation [1, 39, 40]. When activated, both phagocytes exhibit similar morphology and pathophysiological functions. However, our data suggested that the two “twin” phagocytes do not share the same activation pathways after stroke, at least in the case of the IRF4/5 regulatory axis. IRF4/5 are expressed by both microglia and monocytes [1, 3, 7, 8, 28, 41, 42]. Our previous study used IRF4 or IRF5 CKO mice based on the pan-phagocytic Cre system (i.e., lysozyme Cre) and found that CKO of the two IRFs in microglia/monocytes led to an alteration in inflammatory responses only in microglia but not in monocytes [1]. This finding led to our hypothesis that the IRF4-IRF5 regulatory axis may not play a key role in the polarization of infiltrating monocytes in stroke brains. The present study used BM chimera models that can separate central and peripheral molecular signaling and has confirmed our hypothesis by showing that monocytic IRF4/5 have minimal effect on monocyte activation. Of note, the IRF family has a total of 9 members from IRF1 to IRF9 [43–45]. Our study cannot rule out the possibility of other IRFs’ involvement in monocytic activation. The different activation pathways for microglia and monocytes might reflect the different origination of the two phagocytic populations, with the former derived from erythromyeloid precursors in the yolk sac [46] and the latter from hematopoietic stem cells in the bone marrow [47, 48]. The differentiated effects of IRF4/5 on microglia vs. monocyte activation could also be disease type–dependent, as IRFs were reported to play pivotal roles in peripheral macrophage activation in systemic inflammation diseases [49, 50].

We have previously found that IRF4-IRF5 regulatory axis regulates microglial activation in an oscillating manner; that is, CKO of IRF4 led to increased expression of IRF5 and pro-inflammatory response, whereas CKO of IRF5 caused an up-regulated expression of IRF4 and anti-inflammatory response [1]. In the present study, the PB-to-IRF4 or IRF5 CKO chimera cohorts (central IRF manipulation) showed a similar oscillating pattern in microglial response, but the effect was minimal in IRF4 or IRF5 CKO-to-PB cohorts (peripheral IRF manipulation) (Figs. 2 and 3). Ischemic stroke induces microglial activation and peripheral immune cell infiltration into the ischemic brain [51–53]. Interestingly, our data suggested that IRF5 signaling impacts only microglial activation, but IRF4 has broader effects on the activation of both microglia and peripheral immune cells (Fig. 4). This is consistent with our previous study that showed that IRF4 CKO induces significantly more peripheral leukocyte infiltration into the ischemic brain compared to controls, an effect not seen in IRF5 CKO mice [1]. The consistent findings suggest that microglial IRF4 signaling has an inhibitory role in the activation of peripheral leukocytes after stroke, similar to the CD200R inhibitory signaling [54–56]. IRF4 competes with IRF5 for binding to the adaptor protein MyD88 which forms a myddosome together with TNF receptor–associated factor 6, interleukin-1 receptor–associated kinase 1 (IRAK 1), and IRAK 4, for phosphorylation and activation [3, 57]. Whether the competition contributes to the broader effects of IRF4 is not known. Nevertheless, microglial IRF4 and IRF5 signaling both impact stroke outcomes regardless of their differential effects on immune cell activation, indicating that both IRF4 and IRF5 are important in mediating post-stroke inflammation and stroke injury. Of note,

in addition to histological analysis, our stroke outcome assays also include a battery of neurobehavioral tests that evaluated the sensorimotor deficits. Although the histological changes do not necessarily correlate with neurobehavioral deficits [23, 56, 58, 59], the data of the two analyses were consistent with each other in the present study, providing strong evidence that the central IRF4/5 signaling is more important than the peripheral ones (Figs. 5 and 6).

Our data showed that, although central IRF4/5 regulate microglial activation and peripheral IRF4/5 have minimal effect on monocytic activation, both central and peripheral IRF4/5 signaling have a similar effect on brain or plasma cytokine levels (Sup. Figs. 5–8). PB-to-IRF CKO and IRF CKO-to-PB mice yielded a similar pattern of cytokine production, indicating that the cytokine production is independent of phagocytic IRF signaling. This suggests that cytokine production is regulated either by multiple activation pathways in phagocytes or by various immune cells not limited to microglia/monocytes. In addition to IRF signaling, microglial p38 mitogen activated the protein kinase pathway [5, 60], Toll-like receptor 4/NF-κB pathways [61, 62], etc. and also regulates the microglial secretion of inflammatory cytokines. On the other hand, cytokines are not only produced by macrophages but also by lymphocytes, and they can also be produced by polymorphonuclear leukocytes, endothelial and epithelial cells, adipocytes, and connective tissues [63]. Neurons are also a source of cytokine production, including IL-6 [64] and TNF-α [65, 66], and upon ischemic stimulation, these cytokines are released from neurons in large amount. Our previous and present studies showed that microglial IRF signaling impacts stroke outcomes, but the effect may be carried out through multiple microglial functions not limited to cytokine production, including phagocytosis, cytotoxicity, and activation of other immune cells.

To separately study the microglial vs. monocytic IRF4/5 signaling is challenging as the two phagocytic cell populations share almost the same bio-markers, which makes the transgenic CKO method unable to differentiate microglia from monocytes. BM chimera mouse model has been widely used to differentiate central vs. peripheral immune cell signaling [67–70], which is an established technique in this lab. BM reconstitution in the recipient mice resulted in 95% of peripheral immune cells derived from the donor's BM (Fig. 1), indicating the high efficiency of our chimera model. When making the BM chimera model, we shielded the mice's heads with a lead screen to protect the blood–brain barrier [71–74]. Whether the animal head should be shielded or not in the model is somewhat controversial, and one argument is that the BM in the skull will still contribute to hematopoiesis if the head is shielded, and the reconstitution with the donor's BM cells could be "contaminated" by host cells [74, 75]. We have been using the head-shielded method in our previous studies and found that the skull BM did not significantly contribute to the total number of circulating cells, and all our previous experiments were not affected.

The present study has limitations that should be kept in mind when interpreting the data. Due to the complexity of the generation of the bone marrow chimera models (a total of 8 types), we only examined stroke outcomes and post-stroke inflammation at the acute time point (3 days). Although 3 days after MCAO, the induced infarction is already mature [1, 23], and the infiltration of peripheral immune cells also peaks [76–78], it is not known

whether the peripheral IRF4/5 signaling functions at chronic time points (15 days or 30 days), which should be warranted in future studies. Sex is an important variable to consider when designing studies and assessing results; however, in this study, we only included male mice because our pilot study has not found any sex differences in IRF4/5 signaling pre- or post-stroke in WT mice. Nevertheless, this was a chimeric mouse study, and our results were interpreted based on the male chimeras only and not validated for both sexes.

In summary, we generated 8 types of BM chimeras that have been able to distinguish central vs. peripheral IRF4/5 signaling. Although microglia and monocytes both express IRF4/5, the IRF signaling only affects microglial activation. In addition, peripheral leukocyte infiltration into the ischemic brain is regulated by central IRF4 signaling but not by IRF5. Central and peripheral IRF signaling unbiasedly affect cytokine production; however, stroke outcomes are impacted by the central but not peripheral IRF4-IRF5 axis. As microglial IRF4/5 signaling plays a dominant role in post-stroke microglial activation and outcomes, future therapeutic strategies aimed at the intervention of IRF4/5 signaling may only need to target one phagocytic population, i.e., microglia.

Supplementary Material

Refer to Web version on PubMed Central for supplementary material.

Funding

This work was supported by funding from NIH Grants R01 NS093042/NS108779 to Fudong Liu.

Data Availability

The datasets used and/or analyzed in the present study are available from the corresponding author on reasonable request.

Abbreviations

BM	Bone marrow
CD	Cluster of differentiation
cGy	Centigray
CKO	Conditional knockout
CNS	Central nervous system
CV	Cresyl Violet
ELISA	Enzyme-linked immunosorbent assay
fl/fl	Flox
GM-CSF	Granulocyte-macrophage colony-stimulating factor
IRF	Interferon regulatory factor

IL	Interleukin
IL-1β	Interleukin-1 beta
JVI	Jugular vein injection
MCAO	Middle cerebral artery occlusion
M-CSF	Macrophage colony-stimulating factor
MFI	Mean fluorescence intensity
NDS	Neurological deficit scores
PB	PepBoy
PBS	Phosphate-buffered saline
PFA	Paraformaldehyde
TNF-α	Tumor necrosis factor-alpha
RBCs	Red blood cells
RPMI	Roswell Park Memorial Institute
Sup	Supplementary
TAC	Tris-ammonium chloride

References

1. Al Mamun A, Chauhan A, Qi S, Ngwa C, Xu Y, Sharmeen R, Hazen AL, Li J, Aronowski JA, McCullough LD, Liu F. Microglial IRF5-IRF4 regulatory axis regulates neuroinflammation after cerebral ischemia and impacts stroke outcomes. Proc Natl Acad Sci U S A. 2020;117:1742–52. 10.1073/pnas.1914742117. [PubMed: 31892541]
2. Zhang S Microglial activation after ischaemic stroke. Stroke Vasc Neurol. 2019;4:71–4. 10.1136/svn-2018-000196. [PubMed: 31338213]
3. Ngwa C, Mamun AA, Xu Y, Sharmeen R, Liu F. Phosphorylation of microglial IRF5 and IRF4 by IRAK4 regulates inflammatory responses to ischemia. Cells. 2021;10(2):276. 10.3390/cells10020276. [PubMed: 33573200]
4. Zhao SC, Ma LS, Chu ZH, Xu H, Wu WQ, Liu F. Regulation of microglial activation in stroke. Acta Pharmacol Sin. 2017;38:445–58. 10.1038/aps.2016.162. [PubMed: 28260801]
5. Bachstetter AD, Xing B, de Almeida L, Dimayuga ER, Watterson DM, Van Eldik LJ. Microglial p38α MAPK is a key regulator of proinflammatory cytokine up-regulation induced by Toll-like receptor (TLR) ligands or beta-amyloid (Aβ). J Neuroinflammation. 2011;8:79. 10.1186/1742-2094-8-79. [PubMed: 21733175]
6. Bennett ML, Bennett FC, Liddelow SA, Ajami B, Zamanian JL, Fernhoff NB, Mulinyawe SB, Bohlen CJ, Adil A, Tucker A, Weissman IL, Chang EF, Li G, Grant GA, Hayden Gephart MG, Barres BA. New tools for studying microglia in the mouse and human CNS. Proc Natl Acad Sci U S A. 2016;113:E1738–46. 10.1073/pnas.1525528113. [PubMed: 26884166]
7. Ngwa C, Al Mamun A, Qi S, Sharmeen R, Xu Y, Liu F. Regulation of microglial activation in stroke in aged mice: a translational study. Aging (Albany NY). 2022;14:6047–65. 10.18632/aging.204216. [PubMed: 35963621]

8. Corbin AL, Gomez-Vazquez M, Berthold DL, Attar M, Arnold IC, Powrie FM, Sansom SN, Udalova IA. IRF5 guides monocytes toward an inflammatory CD11c(+) macrophage phenotype and promotes intestinal inflammation. Sci Immunol. 2020;5(47). 10.1126/sciimmunol.aax6085.

9. Günthner R, Anders HJ. Interferon-regulatory factors determine macrophage phenotype polarization. Mediators Inflamm. 2013;2013:731023. 10.1155/2013/731023. [PubMed: 24379524]

10. Brune Z, Rice MR, Barnes BJ. Potential T cell-intrinsic regulatory roles for iRF5 via cytokine modulation in T helper subset differentiation and function. Front Immunol. 2020;11:1143. 10.3389/fimmu.2020.01143. [PubMed: 32582209]

11. Gaissmaier L, Elshiaty M, Christopoulos P. Breaking bottlenecks for the TCR therapy of cancer. Cells. 2020;9(9):2095. 10.3390/cells9092095. [PubMed: 32937956]

12. Shafer P, Kelly LM, Hoyos V. Cancer therapy with TCR-engineered T cells: current strategies, challenges, and prospects. Front Immunol. 2022;13:835762. 10.3389/fimmu.2022.835762. [PubMed: 35309357]

13. Venkat P, Shen Y, Chopp M, Chen J. Cell-based and pharmacological neurorestorative therapies for ischemic stroke. Neuropharmacology. 2018;134:310–22. 10.1016/j.neuropharm.2017.08.036. [PubMed: 28867364]

14. Kim H, Cho M, Shim W, Kim J, Jeon E, Kim D, Yoon S. Deficient autophagy in microglia impairs synaptic pruning and causes social behavioral defects. Mol Psychiatry. 2017;22:1576–84. [PubMed: 27400854]

15. Zhang X, Wang Y, Yuan J, Li N, Pei S, Xu J, Luo X, Mao C, Liu J, Yu T. Macrophage/microglial Ezh2 facilitates autoimmune inflammation through inhibition of Socs3. J Exp Med. 2018;215:1365–82. [PubMed: 29626115]

16. Pulido-Salgado M, Vidal-Taboada JM, Garcia Diaz-Barriga G, Serratosa J, Valente T, Castillo P, Matalonga J, Straccia M, Canals JM, Valledor AF. Myeloid C/EBPß deficiency reshapes microglial gene expression and is protective in experimental autoimmune encephalomyelitis. J Neuroinflammation. 2017;14(1):54. [PubMed: 28302135]

17. Shi J, Hua L, Harmer D, Li P, Ren G. Cre driver mice targeting macrophages. Methods Mol Biol. 2018;1784:263–75. 10.1007/978-1-4939-7837-3_24. [PubMed: 29761406]

18. Ritzel RM, Lai YJ, Crapser JD, Patel AR, Schrecengost A, Grenier JM, Mancini NS, Patrizz A, Jellison ER, Morales-Scheihing D, Venna VR, Kofler JK, Liu F, Verma R, McCullough LD. Aging alters the immunological response to ischemic stroke. Acta Neuropathol. 2018;136:89–110. 10.1007/s00401-018-1859-2. [PubMed: 29752550]

19. Ritzel RM, Patel AR, Grenier JM, Crapser J, Verma R, Jellison ER, McCullough LD. Functional differences between microglia and monocytes after ischemic stroke. J Neuroinflammation. 2015;12:106. 10.1186/s12974-015-0329-1. [PubMed: 26022493]

20. Gordan S, Albert H, Danzer H, Lux A, Biburger M, Nimmerjahn F. The immunological organ environment dictates the molecular and cellular pathways of cytotoxic antibody activity. Cell Rep. 2019;29:3033–3046.e4. 10.1016/j.celrep.2019.10.111. [PubMed: 31801071]

21. Bi L, Wacker BK, Stamatikos A, Sethuraman M, Komandur K, Dichek DA. Jugular vein injection of high-titer lentiviral vectors does not transduce the aorta-brief report. Arterioscler Thromb Vasc Biol. 2021;41:1149–55. 10.1161/atvbaha.120.315125. [PubMed: 33297756]

22. de Vasconcelos Dos Santos A, da Costa Reis J, Diaz Paredes B, Moraes L, Jasmin Giraldi-Guimarães A, Mendez-Otero R. Therapeutic window for treatment of cortical ischemia with bone marrow-derived cells in rats. Brain Res. 2010;1306:149–58. 10.1016/j.brainres.2009.09.094. [PubMed: 19799881]

23. Liu F, Schafer DP, McCullough LD. TTC, fluoro-Jade B and NeuN staining confirm evolving phases of infarction induced by middle cerebral artery occlusion. J Neurosci Methods. 2009;179:1–8. [PubMed: 19167427]

24. McCullough LD, Zeng Z, Blizzard KK, Debchoudhury I, Hurn PD. Ischemic nitric oxide and poly (ADP-ribose) polymerase-1 in cerebral ischemia: male toxicity, female protection. J Cereb Blood Flow Metab. 2005;25:502–12. 10.1038/sj.jcbfm.9600059. [PubMed: 15689952]

25. Qi S, Ngwa C, Al Mamun A, Romana S, Wu T, Marrelli SP, Arnold AP, McCullough LD, Liu F. X, but not Y, chromosomal complement contributes to stroke sensitivity in aged animals. Transl Stroke Res. 2022. 10.1007/s12975-022-01070-z.

26. Ritzel RM, Patel AR, Pan S, Crapser J, Hammond M, Jellison E, McCullough LD. Age- and location-related changes in microglial function. Neurobiol Aging. 2015;36:2153–63. 10.1016/j.neurobiolaging.2015.02.016. [PubMed: 25816747]
27. Ritzel RM, Patel AR, Spychala M, Verma R, Crapser J, Koellhoffer EC, Schrecengost A, Jellison ER, Zhu L, Venna VR, McCullough LD. Multiparity improves outcomes after cerebral ischemia in female mice despite features of increased metabovascular risk. Proc Natl Acad Sci U S A. 2017;114:E5673–e5682. 10.1073/pnas.1607002114. [PubMed: 28645895]
28. Al Mamun A, Chauhan A, Yu H, Xu Y, Sharmeen R, Liu F. Interferon regulatory factor 4/5 signaling impacts on microglial activation after ischemic stroke in mice. Eur J Neurosci. 2018;47:140–9. 10.1111/ejn.13778. [PubMed: 29131464]
29. Liu F, Yuan R, Benashski SE, McCullough LD. Changes in experimental stroke outcome across the life span. J Cereb Blood Flow Metab. 2009;29:792–802. 10.1038/jcbfm.20095. [PubMed: 19223913]
30. Li X, Blizzard KK, Zeng Z, DeVries AC, Hurn PD, McCullough LD. Chronic behavioral testing after focal ischemia in the mouse: functional recovery and the effects of gender. Exp Neurol. 2004;187:94–104. 10.1016/j.expneurol.2004.01.004. [PubMed: 15081592]
31. Bouet V, Boulouard M, Toutain J, Divoux D, Bernaudin M, Schumann-Bard P, Freret T. The adhesive removal test: a sensitive method to assess sensorimotor deficits in mice. Nat Protoc. 2009;4:1560–4. [PubMed: 19798088]
32. Ahnstedt H, Patrizz A, Chauhan A, Roy-O'Reilly M, Furr JW, Spychala MS, D'Aigle J, Blixt FW, Zhu L, Bravo Alegria J, McCullough LD. Sex differences in T cell immune responses, gut permeability and outcome after ischemic stroke in aged mice. Brain Behav Immun. 2020;87:556–67. 10.1016/j.bbi.2020.02.001. [PubMed: 32058038]
33. Beeton C, Garcia A, Chandy KG. Drawing blood from rats through the saphenous vein and by cardiac puncture. J Vis Exp. 2007;7:266. 10.3791/266.
34. Qi S, Al Mamun A, Ngwa C, Romana S, Ritzel R, Arnold AP, McCullough LD, Liu F. X chromosome escapee genes are involved in ischemic sexual dimorphism through epigenetic modification of inflammatory signals. J Neuroinflammation. 2021;18:70. 10.1186/s12974-021-02120-3. [PubMed: 33712031]
35. Butturini E, Boriero D, de Prati AC, Mariotto S. STAT1 drives M1 microglia activation and neuroinflammation under hypoxia. Arch Biochem Biophys. 2019;669:22–30. [PubMed: 31121156]
36. Bok E, Chung YC, Kim K-S, Baik HH, Shin W-H, Jin BK. Modulation of M1/M2 polarization by capsaicin contributes to the survival of dopaminergic neurons in the lipopolysaccharide-lesioned substantia nigra in vivo. Exp Mol Med. 2018;50:1–14.
37. Chistiakov DA, Myasoedova VA, Revin VV, Orekhov AN, Bobryshev YV. The impact of interferon-regulatory factors to macrophage differentiation and polarization into M1 and M2. Immunobiology. 2018;223:101–11. 10.1016/j.imbio.2017.10.005. [PubMed: 29032836]
38. Wicks EE, Ran KR, Kim JE, Xu R, Lee RP, Jackson CM. The translational potential of microglia and monocyte-derived macrophages in ischemic stroke. Front Immunol. 2022;13:897022. 10.3389/fimmu.2022.897022. [PubMed: 35795678]
39. Hanisch UK. Microglia as a source and target of cytokines. Glia. 2002;40:140–55. [PubMed: 12379902]
40. Welser-Alves JV, Milner R. Microglia are the major source of TNF-α and TGF-β1 in postnatal glial cultures; regulation by cytokines, lipopolysaccharide, and vitronectin. Neurochem Int. 2013;63:47–53. [PubMed: 23619393]
41. Zhao S-c, Wang C, Xu H, Wu W-q, Chu Z-h, Ma L-s, Z Y-d, Liu F. Age-related differences in interferon regulatory factor-4 and -5 signaling in ischemic brains of mice. Acta Pharmacol Sin. 2017;38:1425–34. 10.1038/aps.2017.122. [PubMed: 28905935]
42. Thompson CD, Matta B, Barnes BJ. Therapeutic targeting of IRFs: pathway-dependence or structure-based? Front Immunol. 2018;9:2622. 10.3389/fimmu.2018.02622. [PubMed: 30515152]
43. Takaoka A, Tamura T, Taniguchi T. Interferon regulatory factor family of transcription factors and regulation of oncogenesis. Cancer Sci. 2008;99:467–78. 10.1111/j.1349-7006.2007.00720.x. [PubMed: 18190617]

44. Taniguchi T, Ogasawara K, Takaoka A, Tanaka N. IRF family of transcription factors as regulators of host defense. Annu Rev Immunol. 2001;19:623–55. 10.1146/annurev.immunol.19.1.623. [PubMed: 11244049]
45. Yanai H, Negishi H, Taniguchi T. The IRF family of transcription factors: inception, impact and implications in oncogenesis. Oncoimmunology. 2012;1:1376–86. 10.4161/onci.22475. [PubMed: 23243601]
46. Kierdorf K, Erny D, Goldmann T, Sander V, Schulz C, Perdiguero EG, Wieghofer P, Heinrich A, Riemke P, Hölscher C, Müller DN, Luckow B, Brocker T, Debowski K, Fritz G, Opdenakker G, Diefenbach A, Biber K, Heikenwalder M, Geissmann F, Rosenbauer F, Prinz M. Microglia emerge from erythromyeloid precursors via Pu.1- and Irf8-dependent pathways. Nat Neurosci. 2013;16:273–80. 10.1038/nn.3318. [PubMed: 23334579]
47. Wolf AA, Yáñez A, Barman PK, Goodridge HS. The ontogeny of monocyte subsets. Front Immunol. 2019;10:1642. 10.3389/fimmu.2019.01642. [PubMed: 31379841]
48. Guilliams M, Mildner A, Yona S. Developmental and functional heterogeneity of monocytes. Immunity. 2018;49:595–613. 10.1016/j.immuni.2018.10.005. [PubMed: 30332628]
49. Parisi L, Gini E, Baci D, Tremolati M, Fanuli M, Bassani B, Farronato G, Bruno A, Mortara L. Macrophage polarization in chronic inflammatory diseases: killers or builders? J Immunol Res. 2018;2018:8917804. 10.1155/2018/8917804. [PubMed: 29507865]
50. Austermann J, Roth J, Barczyk-Kahlert K. The good and the bad: monocytes' and macrophages' diverse functions in inflammation. Cells. 2022;11(12):1979. 10.3390/cells11121979. [PubMed: 35741108]
51. Weinstein JR, Koerner IP, Möller T. Microglia in ischemic brain injury. Future Neurol. 2010;5:227–46. 10.2217/fnl.10.1. [PubMed: 20401171]
52. Berchtold D, Priller J, Meisel C, Meisel A. Interaction of microglia with infiltrating immune cells in the different phases of stroke. Brain Pathol. 2020;30:1208–18. 10.1111/bpa.12911. [PubMed: 33058417]
53. Zhang Z, Lv M, Zhou X, Cui Y. Roles of peripheral immune cells in the recovery of neurological function after ischemic stroke. Front Cell Neurosci. 2022;16:1013905. 10.3389/fncel.2022.1013905. [PubMed: 36339825]
54. van der Vlist M, Ramos MIP, van den Hoogen LL, Hiddingh S, Timmerman LM, de Hond TAP, Kaan ED, van der Kroef M, Lebbink RJ, Peters FMA, Khoury-Hanold W, Fritsch-Stork R, Radstake T, Meyaard L. Signaling by the inhibitory receptor CD200R is rewired by type I interferon. Sci Signal. 2021;14:eabb4324. 10.1126/scisignal.abb4324. [PubMed: 34637328]
55. Vaine CA, Soberman RJ. The CD200-CD200R1 inhibitory signaling pathway: immune regulation and host-pathogen interactions. Adv Immunol. 2014;121:191–211. 10.1016/b978-0-12-800100-4.00005-2. [PubMed: 24388216]
56. Ritzel RM, Al Mamun A, Crapser J, Verma R, Patel AR, Knight BE, Harris N, Mancini N, Roy-O'Reilly M, Ganesh BP, Liu F, McCullough LD. CD200-CD200R1 inhibitory signaling prevents spontaneous bacterial infection and promotes resolution of neuroinflammation and recovery after stroke. J Neuroinflammation. 2019;16:40. 10.1186/s12974-019-1426-3. [PubMed: 30777093]
57. Takaoka A, Yanai H, Kondo S, Duncan G, Negishi H, Mizutani T, Kano S-i, Honda K, Ohba Y, Mak TW. Integral role of IRF-5 in the gene induction programme activated by Toll-like receptors. Nature. 2005;434:243–9. [PubMed: 15665823]
58. Balkaya M, Kröber JM, Rex A, Endres M. Assessing post-stroke behavior in mouse models of focal ischemia. J Cereb Blood Flow Metab. 2013;33:330–8. 10.1038/jcbfm.2012.185. [PubMed: 23232947]
59. Zhou J, Zhuang J, Li J, Ooi E, Bloom J, Poon C, Lax D, Rosenbaum DM, Barone FC. Long-term post-stroke changes include myelin loss, specific deficits in sensory and motor behaviors and complex cognitive impairment detected using active place avoidance. PLoS One. 2013;8:e57503. 10.1371/journal.pone.0057503. [PubMed: 23505432]
60. Bachstetter AD, Van Eldik LJ. The p38 MAP kinase family as regulators of proinflammatory cytokine production in degenerative diseases of the CNS. Aging Dis. 2010;1:199–211. [PubMed: 22720195]

61. Wilms H, Rosenstiel P, Sievers J, Deuschl G, Zecca L, Lucius R. Activation of microglia by human neuromelanin is NF-kappaB dependent and involves p38 mitogen-activated protein kinase: implications for Parkinson's disease. Faseb J. 2003;17:500–2. 10.1096/fj.02-0314fje. [PubMed: 12631585]
62. Shi Y, Zhang L, Teng J, Miao W. HMGB1 mediates microglia activation via the TLR4/NF-κB pathway in coriaria lactone induced epilepsy. Mol Med Rep. 2018;17:5125–31. 10.3892/mmr.2018.8485. [PubMed: 29393419]
63. Arango Duque G, Descoteaux A. Macrophage cytokines: involvement in immunity and infectious diseases. Front Immunol. 2014;5:491. 10.3389/fimmu.2014.00491. [PubMed: 25339958]
64. Erta M, Quintana A, Hidalgo J. Interleukin-6, a major cytokine in the central nervous system. Int J Biol Sci. 2012;8:1254–66. 10.7150/ijbs.4679. [PubMed: 23136554]
65. Park KM, Bowers WJ. Tumor necrosis factor-alpha mediated signaling in neuronal homeostasis and dysfunction. Cell Signal. 2010;22:977–83. 10.1016/j.cellsig.2010.01.010. [PubMed: 20096353]
66. Liu T, Clark RK, McDonnell PC, Young PR, White RF, Barone FC, Feuerstein GZ. Tumor necrosis factor-alpha expression in ischemic neurons. Stroke. 1994;25:1481–8. 10.1161/01.str.25.7.1481. [PubMed: 8023366]
67. Hodes GE, Pfau ML, Leboeuf M, Golden SA, Christoffel DJ, Bregman D, Rebusi N, Heshmati M, Aleyasin H, Warren BL, Lebonté B, Horn S, Lapidus KA, Stelzhammer V, Wong EH, Bahn S, Krishnan V, Bolaños-Guzman CA, Murrough JW, Merad M, Russo SJ. Individual differences in the peripheral immune system promote resilience versus susceptibility to social stress. Proc Natl Acad Sci U S A. 2014;111:16136–41. 10.1073/pnas.1415191111. [PubMed: 25331895]
68. Yu K, Youshani AS, Wilkinson FL, O'Leary C, Cook P, Laaniste L, Liao A, Mosses D, Waugh C, Shorrock H, Pathmanaban O, Macdonald A, Kamaly-Asl I, Roncaroli F, Bigger BW. A nonmyeloablative chimeric mouse model accurately defines microglia and macrophage contribution in glioma. Neuropathol Appl Neurobiol. 2019;45:119–40. 10.1111/nan.12489. [PubMed: 29679380]
69. Achyut BR, Shankar A, Iskander AS, Ara R, Knight RA, Scicli AG, Arbab AS. Chimeric mouse model to track the migration of bone marrow derived cells in glioblastoma following anti-angiogenic treatments. Cancer Biol Ther. 2016;17:280–90. 10.1080/15384047.2016.1139243. [PubMed: 26797476]
70. Tashima R, Mikuriya S, Tomiyama D, Shiratori-Hayashi M, Yamashita T, Kohro Y, Tozaki-Saitoh H, Inoue K, Tsuda M. Bone marrow-derived cells in the population of spinal microglia after peripheral nerve injury. Sci Rep. 2016;6:23701. 10.1038/srep23701. [PubMed: 27005516]
71. Müller A, Brandenburg S, Turkowski K, Müller S, Vajkoczy P. Resident microglia, and not peripheral macrophages, are the main source of brain tumor mononuclear cells. Int J Cancer. 2015;137:278–88. 10.1002/ijc.29379. [PubMed: 25477239]
72. Youshani AS, Rowlston S, O'Leary C, Forte G, Parker H, Liao A, Telfer B, Williams K, Kamaly-Asl ID, Bigger BW. Non-myeloablative busulfan chimeric mouse models are less pro-inflammatory than head-shielded irradiation for studying immune cell interactions in brain tumours. J Neuroinflammation. 2019;16:25. 10.1186/s12974-019-1410-y. [PubMed: 30722781]
73. Larochelle A, Bellavance MA, Michaud JP, Rivest S. Bone marrow-derived macrophages and the CNS: an update on the use of experimental chimeric mouse models and bone marrow transplantation in neurological disorders. Biochim Biophys Acta. 2016;1862:310–22. 10.1016/j.bbadis.2015.09.017. [PubMed: 26432480]
74. Krishnan S, Wemyss K, Prise IE, McClure FA, O'Boyle C, Bridgeman HM, Shaw TN, Grainger JR, Konkel JE. Hematopoietic stem and progenitor cells are present in healthy gingiva tissue. J Exp Med. 2021;218(4). 10.1084/jem.20200737.
75. Cugurra A, Mamuladze T, Rustenhoven J, Dykstra T, Beroshvili G, Greenberg ZJ, Baker W, Papadopoulos Z, Drieu A, Blackburn S, Kanamori M, Brioschi S, Herz J, Schuettpelz LG, Colonna M, Smirnov I, Kipnis J. Skull and vertebral bone marrow are myeloid cell reservoirs for the meninges and CNS parenchyma. Science. 2021;373(6553). 10.1126/science.abf7844.
76. Kim E, Yang J, Beltran CD, Cho S. Role of spleen-derived monocytes/macrophages in acute ischemic brain injury. J Cereb Blood Flow Metab. 2014;34:1411–9. 10.1038/jcbfm.2014.101. [PubMed: 24865998]

77. Wattananit S, Tornero D, Graubardt N, Memanishvili T, Monni E, Tatarishvili J, Miskinyte G, Ge R, Ahlenius H, Lindvall O, Schwartz M, Kokaia Z. Monocyte-derived macrophages contribute to spontaneous long-term functional recovery after stroke in mice. J Neurosci. 2016;36:4182–95. 10.1523/jneurosci.4317-15.2016. [PubMed: 27076418]

78. Garcia-Bonilla L, Faraco G, Moore J, Murphy M, Racchumi G, Srinivasan J, Brea D, Iadecola C, Anrather J. Spatio-temporal profile, phenotypic diversity, and fate of recruited monocytes into the post-ischemic brain. J Neuroinflammation. 2016;13:285. 10.1186/s12974-016-0750-0. [PubMed: 27814740]

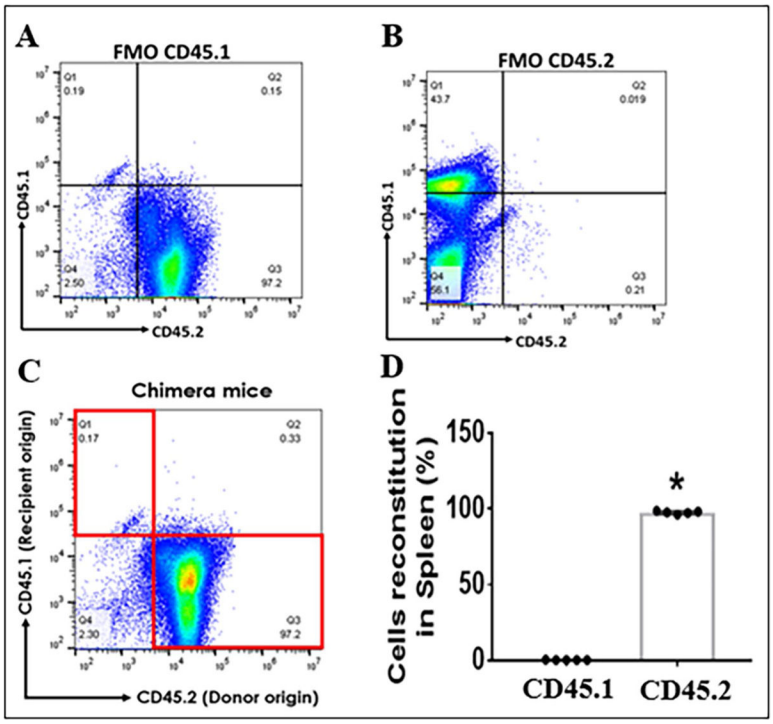

Fig. 1.

Validation of BM chimeric mice with flow cytometry on spleen cells. **A** Fluorescence minus one (FMO) positive threshold for CD45.1^{+} spleen cells. **B** FMO for CD45.2.$^{+}$ spleen cells. **C** CD45.1 (recipient) and .2 (donor) gating plot for spleen cells in a representative chimeric mouse. **D** quantitative flow data of the spleen cells in (**C**). $n = 5–7$ per group; $*P < 0.05$

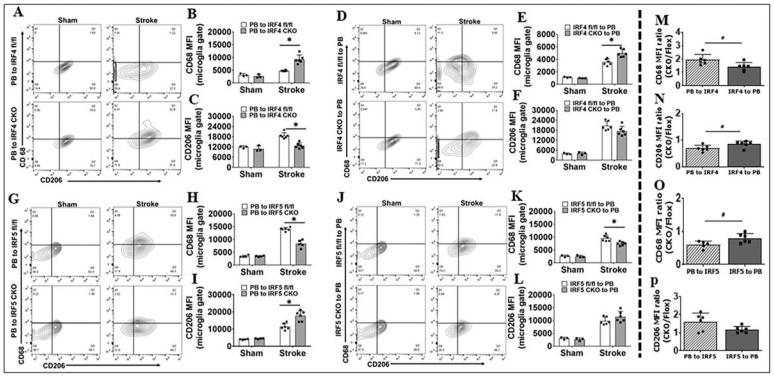

Fig. 2.

Microglial cell membrane inflammatory markers (CD68 and CD206) in BM chimera analyzed by flow cytometry 3 days after MCAO. Representative flow plots showing $CD68^{+}$ and $CD206.^{+}$ cells in **A** PB-to-IRF4 (CKO and flox), **D** IRF4 (CKO and flox)-to-PB, **G** PB-to-IRF5 (CKO and flox), and **J** IRF5 (CKO and flox)-to-PB chimeras. Quantification of CD68 and CD206 MFI for **A** in **B**, **C**; for **D** in **E**, **F**; for **G** in **H**, **I**; and for **J** in **K**, **L**. The MFI ratios of PB-to-IRF CKO/PB-to-IRF flox (PB to IRF) and IRF CKO-to-PB/IRF flox-to-PB (IRF to PB) in stroke groups are compared in **M** for **B** and **E**, in **N** for **C** and **F**, in **O** for **H** and **K**, and in **P** for **I** and **L**. $n = 3–4$ per sham and $n = 6$ per stroke group; $*P < 0.05$

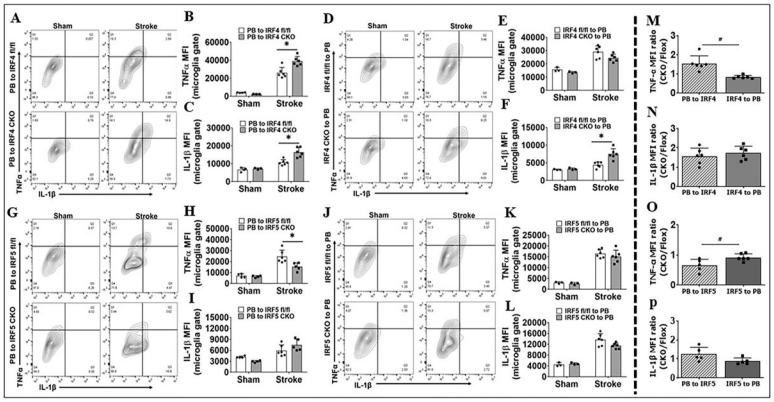

Fig. 3.

Microglial intracellular inflammatory markers (TNF-α and IL-1β) in BM chimera analyzed by flow cytometry 3 days after MCAO. Representative flow plots showing TNF-α^+ and IL-1β.$^+$ cells in **A** PB-to-IRF4 (CKO and flox), **D** IRF4 (CKO and flox)-to-PB, **G** PB-to-IRF5 (CKO and flox), and **J** IRF5 (CKO and flox)-to-PB chimeras. Quantification of TNF-α and IL-1β MFI for **A** in **B**, **C**; for **D** in **E**, **F**; for **G** in **H**, **I**; and for **J** in **K**, **L**. The MFI ratios of PB-to-IRF CKO/PB-to-IRF flox (PB to IRF) and IRF CKO-to-PB/IRF flox-to-PB (IRF to PB) in stroke groups are compared in **M** for **B** and **E**, in **N** for **C** and **F**, in **O** for **H** and **K**, in **P** for **I** and **L**. n = 3–4 per sham and n = 6 per stroke group; *$P < 0.05$

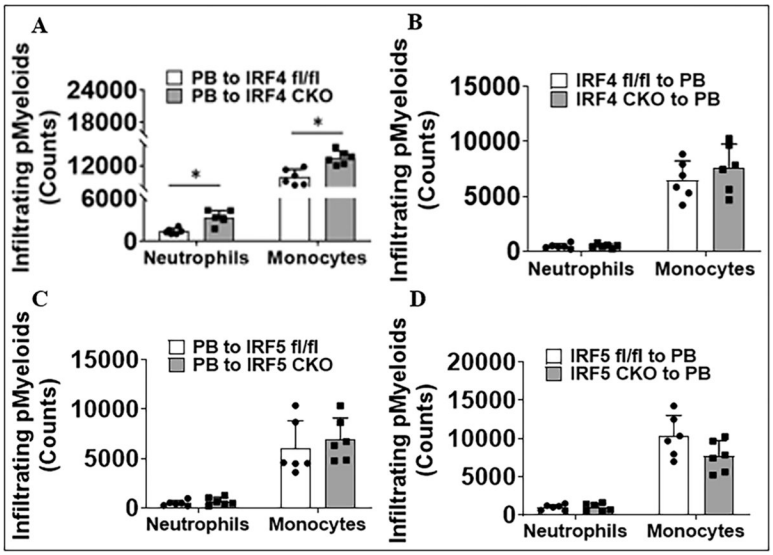

Fig. 4.

Quantification of peripheral myeloid (pMyeloid) immune cell (neutrophils and monocytes) infiltration in ischemic brains of chimeras 3 days after MCAO. **A** IRF4 CKO and flox mice that received BM cells from PB mice. **B** PB mice that received BM cells from IRF4 CKO and flox mice. **C** IRF5 CKO and flox mice that received BM cells from PB mice. **D** PB mice that received BM cells from IRF5 CKO and flox mice. $n = 6$ per group; $*P < 0.05$

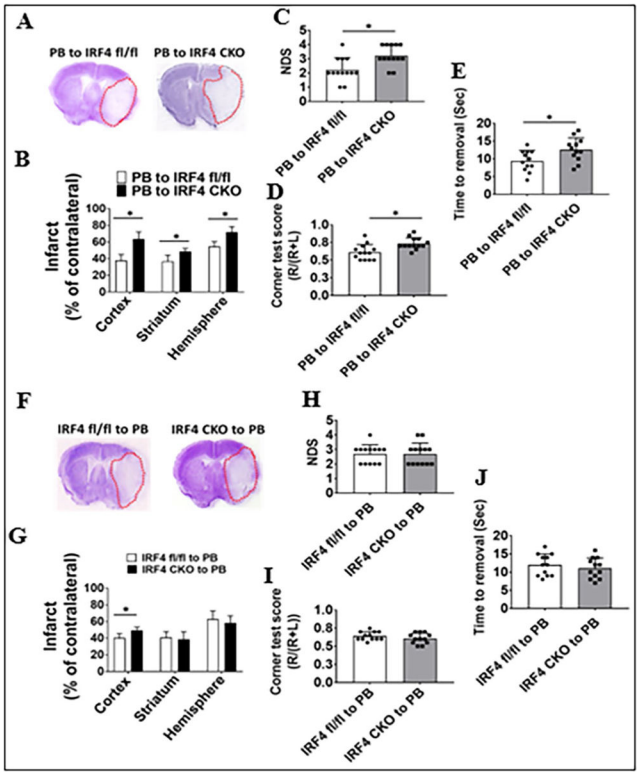

Fig. 5.

Stroke outcomes in IRF4 CKO and flox BM chimeras 3 days after MCAO. Data from chimeras of PB-to-IRF4 flox and CKO are presented (**A**–**E**) and data from chimeras of IRF4 flox and CKO-to-PB (**F**–**J**): **A**, **F** representative brain slices stained with Cresyl violet; infarct areas (white color) were circled with red dotted lines. **B**, **G** Quantification of infarct volumes. **C**, **H** Neurological deficits scores (NDS). **D**, **I** Corner test scores calculated by $R/(R + L) \times 100$, where R and L indicate right and left turn number respectively. **E**, **J** Tape removal test. $n = 6–7$ per group for CV staining, NDS, and corner tests. $n = 12–13$ per group for tape removal test. $^*P < 0.05$

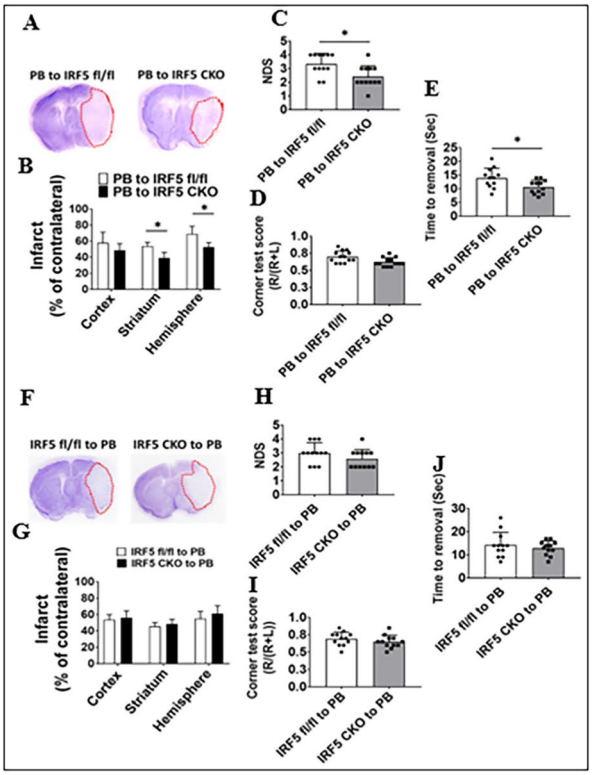

Fig. 6.

Stroke outcomes in IRF5 CKO and flox BM chimeras 3 days after MCAO. Data from chimeras of PB-to-IRF5 flox and CKO are presented (**A**–**E**) and data from chimeras of IRF5 flox and CKO-to-PB **(F**–**J**): **A**, **F** representative brain slices stained with Cresyl violet; infarct areas (white color) were circled with red dotted lines. **B**, **G** Quantification of infarct volumes. **C**, **H** Neurological deficit scores (NDS). **D**, **I** Corner test scores calculated by $R/(R + L) \times 100$, where R and L indicate right and left turn number respectively. **E**, **J** Tape removal test. $n = 6$–7 per group for CV staining, NDS, and corner tests. $n = 12$–13 per group for tape removal test. $^{*}P < 0.05$

Table 1

Types of chimeric mice and experimental grouping. A total of 8 types of chimeras. fl/fl, flox/flox; CKO, conditional knockout

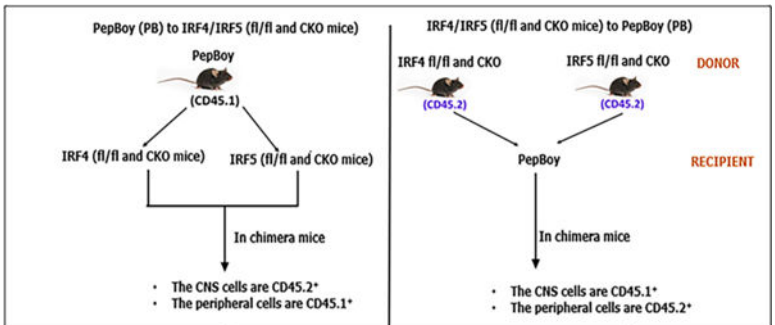

PB (donor) to IRF4 fl/fl (recipient)	Peripheral IRF4 intact vs. Central IRF4 CKO	IRF4 fl/fl (donor) to PB (recipient)	Peripheral IRF4 CKO vs. Central IRF4 intact
PB (donor) to IRF4 CKO (recipient)		IRF4 CKO (donor) to PB (recipient)	
PB (donor) to IRF5 fl/f/ (recipient)	Peripheral IRF5 intact vs. Central IRF4 CKO	IRF5 fl/fl (donor) to PB (recipient)	Peripheral IRF5 CKO vs. Central IRF5 intact
PB (donor) to IRF5 CKO (recipient)		IRF5 CKO (donor) to PB (recipient)	